AIMS Mathematics, 7(9): 15714–15740.
DOI: 10.3934/math.2022861
Received: 31 December 2021
Revised: 02 June 2022
Accepted: 07 June 2022
Published: 24 June 2022

http://www.aimspress.com/journal/Math

Research article

The chaotic mechanisms in some jerk systems

Xiaoyan Hu[1], **Bo Sang**[1,*] **and Ning Wang**[2]

[1] School of Mathematical Sciences, Liaocheng University, Liaocheng 252059, China
[2] School of Electrical and Information Engineering, Tianjin University, Tianjin 300072, China

* **Correspondence:** Email: sangbo_76@163.com.

Abstract: In this work, a five-parameter jerk system with one hyperbolic sine nonlinearity is proposed, in which ε is a small parameter, and a, b, c, d are some other parameters. For $\varepsilon = 0$, the system is Z_2 symmetric. For $\varepsilon \neq 0$, the system loses the symmetry. For the symmetrical case, the pitchfork bifurcation and Hopf bifurcation of the origin are studied analytically by Sotomayor's theorem and Hassard's formulas, respectively. These bifurcations can be either supercritical or subcritical depending on the governing parameters. In comparison, it is much more restrictive for the origin of the Lorenz system: Only a supercritical pitchfork bifurcation is available. Thus, the symmetrical system can exhibit very rich local bifurcation structures. The continuation of local bifurcations leads to the main contribution of this work, i.e., the discovery of two basic mechanisms of chaotic motions for the jerk systems. For four typical cases, Cases A–D, by varying the parameter a, the mechanisms are identified by means of bifurcation diagrams. Cases A and B are Z_2 symmetric, while Cases C and D are asymmetric (caused by constant terms). The forward period-doubling routes to chaos are observed for Cases A and C; meanwhile, the backward period-doubling routes to chaos are observed for Cases B and D. The dynamical behaviors of these cases are studied via phase portraits, two-sided Poincaré sections and Lyapunov exponents. Using Power Simulation (PSIM), a circuit simulation model for a chaotic jerk system is created. The circuit simulations match the results of numerical simulations, which further validate the dynamical behavior of the jerk system.

Keywords: chaos; limit cycle; Hopf bifurcation; pitchfork bifurcation
Mathematics Subject Classification: 34C05, 34C07, 34C23, 34C28, 34C29

1. Introduction

Chaos theory is a very important domain in mathematics, with a variety of applications. It has been applied to disease control and prevention [1], mechanics [2], biology [3], secure communications [4], and many other disciplines. Even small changes in a chaotic system's initial conditions can result in

complex and unpredictable behavior. In the past few decades, many systems with chaotic attractors have been discovered, such as the Lorenz system [5], the Rössler system [6], the Chen system [7], the Yang systems [8] and the Sprott systems [9].

The study of chaotic flows with various equilibrium types is an interesting topic; see [10, 11] and the references therein. In [10], some chaotic systems with a unique equilibrium were presented, admitting various equilibrium types. In the review paper [11], the authors classified chaotic systems with special equilibrium properties into eight groups: systems with no equilibrium (NE), systems with stable equilibrium (SE), systems with line equilibrium (LE), systems with curve equilibrium (CE), systems with plane equilibrium (PE), systems with surface equilibrium (ES), systems with unstable equilibrium (US) and systems that fall into more than one category (Chameleon systems).

Since the seminal work of Leonov et al. [12], the attractors in dynamical systems have been categorized into two categories: self-excited and hidden. A self-excited attractor has a basin of attraction that is associated with an unstable equilibrium. Conversely, an attractor is called hidden if its basin of attraction does not intersect with a small neighborhood of any equilibrium point. The study of systems with hidden attractors has become a popular trend because hidden attractors play a significant role in many theoretical problems and engineering applications. Hidden attractors can be generated by a system in the following four types: Type 1, systems without equilibrium points [13]; Type 2, systems with only stable equilibrium points [14]; Type 3, systems with an infinite number of equilibrium points [15, 16]; Type 4, systems with coexisting self-excited attractors [17].

It is well known that the presence of hidden attractors is connected with multistability [18–21]. For a compass-gait robot model with multistability, Zavareh et al. [21] found that the strange attractors were hidden by the help of a basin of attractions. The concept of perpetual points refers to points where a system's acceleration becomes zero, but its velocity remains nonzero. In some situations, these points may be useful for locating attractors, comprehending dynamics and determining whether the system is conservative or not. For the definition, existence, properties and applications of perpetual points; see [22–25]. Nowadays, the transmission of data with security is an important topic. Encryption with chaos is based on the ability of some dynamic systems to produce a sequence of bits that appear to be random in nature. Recently, a novel chaotic system was presented in [26] with a unique feature of crossing inside and outside of a cylinder repeatedly. Using a novel chaotic system with a hidden attractor, an encryption algorithm was designed in [27] for image encryption.

In a given system, multistability refers to the superposition of several different attractors with the same set of parameters, starting from different initial conditions. A particular feature of multistable systems is their sensitivity to initial conditions. This type of system has a wide variety of states, giving it a great deal of flexibility to meet the needs of different applications [28]. In recent years, considerable attention has been attracted to chaotic systems with multistability. The phenomenon of multistability has been observed in various fields of science, such as secure communications [4], image processing [29], neural systems [30] and economic systems [31]. Extreme multistability means the coexistence of infinitely many attractors; see [32]. Megastability refers to the coexistence of nested infinite attractors; see [33].

As the special case of 3D flows, jerk systems are very attractive due to simple form and theoretical and practical importance. In the recent years, although great efforts have been paid to them, the forming mechanisms of attractors are still far from complete. In fact, one of main problems of bifurcation theory is to understand the transition to chaos.

In physics, jerk is the third derivative of position with respect to time. Therefore, differential equations of the form

$$\dddot{x} = J(x, \dot{x}, \ddot{x}) \tag{1.1}$$

are called jerk equations, where the dot denotes differentiation with respect to time t. The term "jerk" comes from the fact that in a mechanical system, in which x is the displacement, $\dot{x}$ is the velocity, and $\ddot{x}$ is the acceleration, the quantity $\dddot{x}$ is called the "jerk". The jerk function $J(x, \dot{x}, \ddot{x})$ corresponds to a force F per unit mass that satisfies

$$\frac{dF}{dt} = J(x, \dot{x}, \ddot{x}).$$

Letting $y = \dot{x}, z = \ddot{x}$, Eq (1.1) can be transformed into the jerk system:

$$\begin{cases} \dfrac{dx}{dt} = y, \\ \dfrac{dy}{dt} = z, \\ \dfrac{dz}{dt} = J(x, y, z). \end{cases}$$

Many chaotic jerk systems can be found with various forms of $J(x, y, z)$, such as piecewise nonlinear functions, trigonometric functions, absolute value functions or power functions; for more information see [9]. For polynomial jerk systems, the regular and chaotic behavior was studied in [34–37]. In these studies, the qualitative features of equilibria played an important role in determining the complex behavior of the system.

The differential system in the form

$$\begin{cases} \dfrac{dx_1}{dt} = x_2, \\ \dfrac{dx_2}{dt} = x_3, \\ \qquad \vdots \\ \dfrac{dx_n}{dt} = J(x_1, x_2, \cdots, x_n), \end{cases}$$

is called a hyperjerk sytem, where $n > 3$. Due to their simplicity and complex dynamic properties, such systems have received considerable attention. For some hyperjerk systems with $n = 4, 5$, there are many studies on bifurcation analysis, numerical analysis, synchronizations and circuit implementations in [38–43] and references therein. As an exciting field of chaos, hidden attractors of 4D hyperjerk systems were investigated in [40, 42].

Joshi and Ranjan [44] introduced a jerk equation,

$$\dddot{x} + \beta\, \ddot{x} + (\alpha + 1)\beta\, \dot{x} \pm \alpha\beta\gamma\, \sinh(x) = 0, \tag{1.2}$$

where $\alpha > 0, \beta > 0, \gamma > 0$. It possesses a wide variety of behaviors: self-excited or hidden chaos [12]. For the jerk equation

$$\dddot{x} - a\, x + b\, \dot{x} + \ddot{x} + \cosh(x) = 0,$$

Rajagopal et al. [45] found various dynamical behaviors: periodic attractors, one-scroll chaotic attractors and coexistence between chaotic and periodic attractors. Volos et al. [46] presented a new jerk equation,

$$\dddot{x} + x + b\,\ddot{x} + a\,\sinh(\dot{x}) = 0,$$

which exhibits many interesting chaotic phenomena, such as coexisting attractors and antimonotonicity. Kengne et al. [47] considered the dynamics of a novel jerk system, which can be rewritten as

$$\begin{cases} \dfrac{dx}{dt} = y, \\ \dfrac{dy}{dt} = \sigma\, z, \\ \dfrac{dz}{dt} = x - \gamma\, y - z - \varepsilon\,\sinh(\rho x). \end{cases}$$

Using bifurcation analysis, it was found that the system exhibits a period-doubling route to chaos, symmetry recovering crises and multistability. Kengne et al. [48] presented a jerk system, which can be rewritten as

$$\begin{cases} \dfrac{dx}{dt} = y, \\ \dfrac{dy}{dt} = a\, z, \\ \dfrac{dz}{dt} = -\gamma\, y - \mu\, z + \phi_k(x), \end{cases}$$

where

$$\phi_k(x) = -k - 3\,(x - 2\,\tanh(x)).$$

Some unusual and striking nonlinear phenomena were observed in the system: coexisting bifurcation branches, hysteretic dynamics, coexisting asymmetric bubbles, critical transitions and multiple coexisting asymmetric attractors. Li et al. [49] considered a cubic jerk system,

$$\begin{cases} \dfrac{dx}{dt} = y, \\ \dfrac{dy}{dt} = a\, z, \\ \dfrac{dz}{dt} = -x - b\, z + xy^2 - c\, x^2 z - x^3, \end{cases}$$

for which the rich dynamical behaviors were observed, such as period-doubling bifurcation and reverse period-doubling bifurcation routes to chaos, crisis, multiple symmetric coexisting attractors and antimonotonicity.

There are a few jerk systems in the literature which exhibit hidden chaotic attractors. Some of them are listed as follows. For hidden chaotic systems with one stable equilibrium, see cases SE1-SE6 in [50]. More examples can be found in [51–53]. For hidden chaotic systems without equilibrium, see cases NE3, NE6, NE14, NE15 in [54]. Some other examples can be found in [55, 56].

This paper is organized as follows. In the next section, four jerk systems with hyperbolic sine nonlinearity are presented, in which Cases A and C are Z_2 symmetric, and Cases B and D are asymmetric. In Sections 3 and 4, two mechanisms for chaos are studied via bifurcation diagrams,

Poincaré cross sections, phase portraits and Lyapunov exponents. Section 5 is devoted to the local bifurcation analysis for a general jerk system, which includes Cases A and B. In Section 6, the electronic circuit for a chaotic jerk system is designed and simulated through PSIM 9.0.3. The outputs show good agreement with the numerical outputs. Finally, some concluding remarks are drawn in the last section.

2. The jerk systems

Consider the following equation:

$$\dddot{x} + a\,x + b^2\,\dot{x} + c\,\ddot{x} - d\,\sinh(x) = \varepsilon, \tag{2.1}$$

where $0 \le \varepsilon \ll 1$, $b > 0$. It is a generalization of Eq (1.2) since $a,\ b,\ c,\ d$ and ε are independent parameters. In fact, by setting

$$a = \beta,\ b^2 = (\alpha+1)\beta,\ c = 0,\ d = \mp\alpha\beta\gamma,\ \varepsilon = 0$$

in (2.1), we can get (1.2).

Letting $y = \dot{x}$, $z = \ddot{x}$, Eq (2.1) can be transformed into the following jerk system:

$$\begin{cases} \dfrac{dx}{dt} = y, \\ \dfrac{dy}{dt} = z, \\ \dfrac{dz}{dt} = \varepsilon - a\,x - b^2\,y - c\,z + d\,\sinh(x). \end{cases} \tag{2.2}$$

The system is elegant with a nonlinearity in the third equation, which has great influence on the long-term behavior.

2.1. The symmetric case with $\varepsilon = 0$

Letting $\varepsilon = 0$, system (2.2) becomes

$$\begin{cases} \dfrac{dx}{dt} = y, \\ \dfrac{dy}{dt} = z, \\ \dfrac{dz}{dt} = -a\,x - b^2\,y - c\,z + d\,\sinh(x). \end{cases} \tag{2.3}$$

It is Z_2 symmetric with respect to the origin, i.e., if $(x(t), y(t), z(t))$ is a solution of this system, then $(-x(t), -y(t), -z(t))$ is also a solution. Under some appropriate conditions, the symmetry can produce a single symmetric attractor or a symmetric pair of attractors.

The system is conservative if $c = 0$, the system is explosive if $c < 0$, and the system is dissipative if $c > 0$. From now on, we assume that

$$b > 0, \quad c > 0, \quad d \neq 0. \tag{2.4}$$

Thus, the system is dissipative with a negative divergence $\nabla V = -c$, i.e., the flow of the system uniformly contracts the volumes of the state space, and all orbits of the system are eventually confined to a specific subset of zero volume.

To understand the chaotic mechanisms of system (2.3), the following two special cases are mainly considered in the next two sections:

$$\text{Case A}: \begin{cases} \dfrac{dx}{dt} = y, \\ \dfrac{dy}{dt} = z, \\ \dfrac{dz}{dt} = -a\,x - y - 0.2\,z + \sinh(x), \end{cases} \tag{2.5}$$

and

$$\text{Case B}: \begin{cases} \dfrac{dx}{dt} = y, \\ \dfrac{dy}{dt} = z, \\ \dfrac{dz}{dt} = -a\,x - y - 0.2\,z - \sinh(x). \end{cases} \tag{2.6}$$

It should be remarked that, although these two systems are very special, the underlying mechanisms can also be found in many other jerk systems, such as the following polynomial jerk systems:

$$\begin{cases} \dfrac{dx}{dt} = y, \\ \dfrac{dy}{dt} = z, \\ \dfrac{dz}{dt} = -a\,x - y - 0.2\,z + x^3, \end{cases}$$

$$\begin{cases} \dfrac{dx}{dt} = y, \\ \dfrac{dy}{dt} = z, \\ \dfrac{dz}{dt} = -a\,x - y - 0.2\,z - x^3. \end{cases}$$

2.2. The asymmetric case with $\varepsilon = 0.01$

Letting $\varepsilon = 0.01$, system (2.2) becomes

$$\begin{cases} \dfrac{dx}{dt} = y, \\ \dfrac{dy}{dt} = z, \\ \dfrac{dz}{dt} = 0.01 - a\,x - b^2\,y - c\,z + d\,\sinh(x), \end{cases} \tag{2.7}$$

which is an asymmetric jerk system.

To understand the chaotic mechanisms of system (2.7), the following two special cases are also considered in the next two sections:

$$\text{Case C}: \begin{cases} \dfrac{dx}{dt} = y, \\ \dfrac{dy}{dt} = z, \\ \dfrac{dz}{dt} = 0.01 - a\,x - y - 0.2\,z + \sinh(x), \end{cases} \tag{2.8}$$

and

$$\text{Case D}: \begin{cases} \dfrac{dx}{dt} = y, \\ \dfrac{dy}{dt} = z, \\ \dfrac{dz}{dt} = 0.01 - a\,x - y - 0.2\,z - \sinh(x). \end{cases} \tag{2.9}$$

3. Mechanism I: forward period-doubling route to chaos

This section is about the dynamical analysis and bifurcation analysis of Cases A and C. For these systems, the bifurcation diagrams will be plotted, depicting the local maxima of $x(t)$ versus the parameter a. It would be interesting to see that the underlying mechanisms are the same: forward period-doubling routes to chaos.

A set of six initial conditions are selected as candidates: $S_i : (x, y, z) = (0, 0, m_i), \quad 1 \le i \le 6$, where

$$m_{1,2} = \pm 0.1, \quad m_{3,4} = \pm 1, \quad m_{5,6} = \pm 0.8. \tag{3.1}$$

3.1. Case A

With the initial conditions $S_{1,2}$, the bifurcation diagram of system (2.5) with respect to the parameter a is plotted in Figure 1. Here, the blue branches correspond to S_1, and the red branches correspond to S_2.

Due to Z_2 symmetry, we only describe the long term behaviors of the trajectory starting from the point S_1, corresponding to the blue branches in Figure 1. When the parameter a varies from 1.1 to 1.67, the system displays a stable equilibrium up to $a = 1.2$, where the supercritical Hopf bifurcation triggers a period-1 limit cycle. For $1.2 < a < 1.4$, the amplitude of the cycle grows with the increase of a. For $1.4 < a < 1.58$, the fluctuations of the amplitude with jumps can be observed. At about $a = 1.58$, the cycle exhibits the first period-doubling bifurcation. With further increase in parameter a, the system shows a period-doubling route to chaotic oscillations. For $1.618 \le a \le 1.67$, the system enters a chaotic state. Furthermore, the corresponding Lyapunov exponents versus a are shown in Figure 2, in which the initial conditions correspond to S_1. In Figure 2, stable equilibrium corresponds to the largest Lyapunov exponent L_1 that is less than zero, periodic dynamics correspond to L_1 that is equal to zero, and chaotic behavior corresponds to L_1 that is greater than zero. The bifurcation diagram and the Lyapunov exponent spectrum are in very good agreement.

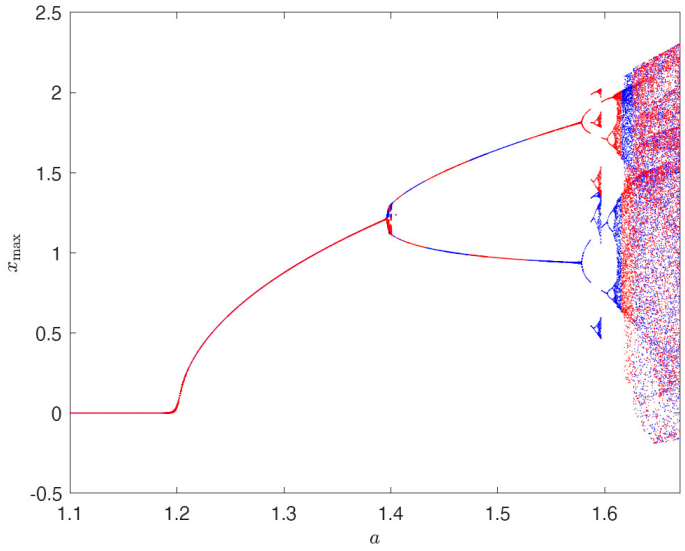

Figure 1. The bifurcation diagram of system (2.5) for $a \in [1.1, 1.67]$. Initial conditions: S_1 (blue), S_2 (red).

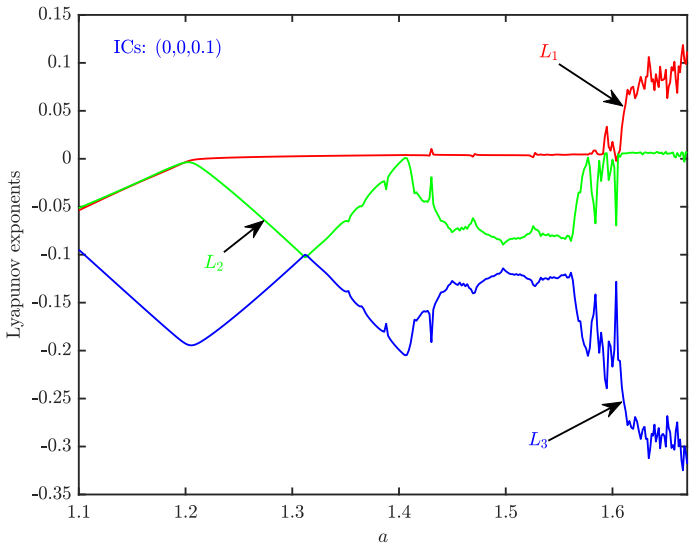

Figure 2. Lyapunov exponent spectrum of system (2.5) for $a \in [1.1, 1.67]$.

In fact, a subcritical pitchfork bifurcation also occurs at the origin for $a = 1$, which is out of the scope of this section. For more details about the local bifurcations, see Section 5.

For $a = 1.3, 1.5, 1.605$, the 2D views of the periodic attractors are shown in Figure 3.

The coexistence of chaotic attractors can be found at $a = 1.618$; see Figure 4.

A fully developed one-scroll chaotic attractor can be found at $a = 1.67$, which is shown in Figure 5.

To illustrate the folding and stretching structure of the attractor, cross sections (two-sided Poincaré sections) are plotted in Figure 6. If the parameter a is further increased, we see that a boundary crisis

occurs at $a = 1.6777$.

The 3D chaotic attractors of the system for $a = 1.618$ and $a = 1.67$ are plotted in Figure 7. For the latter chaotic attractor, the Lyapunov exponents are 0.1071, 0, -0.3071, and thus the Kaplan-Yorker dimension is $D_{\mathrm{KY}} = 2.3487$.

With the other initial conditions S_3–S_6 and $a \in [1.58, 1.59]$, the bifurcation diagram of system (2.5) is plotted in Figure 8, which illustrates the domain of the coexistence of multiple periodic attractors. Here, the blue branches correspond to S_3, the red branches correspond to S_4, the green branches correspond to S_5, and the black branches correspond to S_6. For $a = 1.584$, two period-2 and two period-3 limit cycles can be observed in Figure 8.

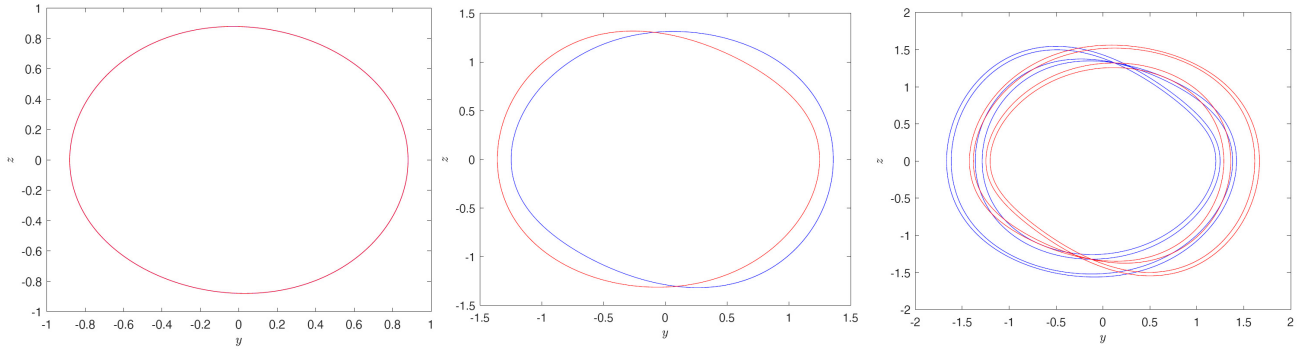

(a) $a = 1.3$ **(b)** $a = 1.5$ **(c)** $a = 1.605$

Figure 3. Periodic attractors of system (2.5) for $a = 1.3, 1.5$ and 1.605. Initial conditions: S_1 (blue), S_2 (red).

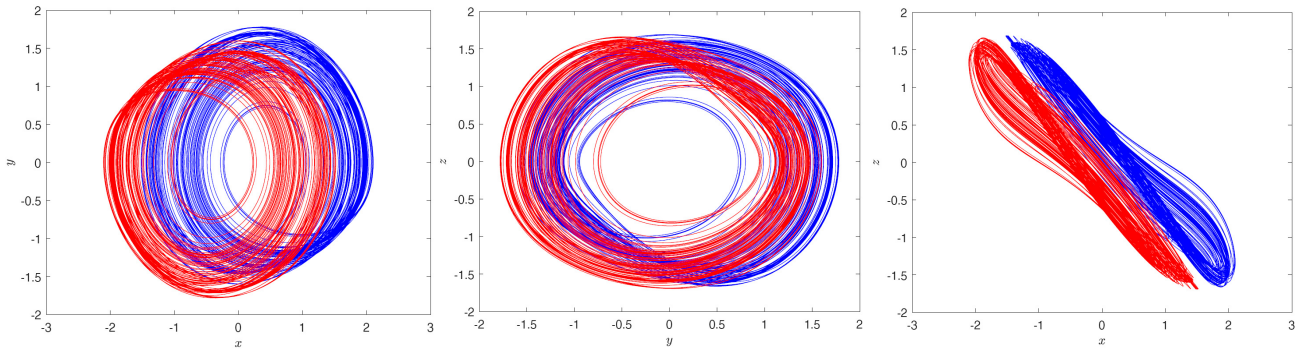

(a) $x - y$ plane **(b)** $y - z$ plane **(c)** $x - z$ plane

Figure 4. 2D views of the chaotic attractors of system (2.5) for $a = 1.618$. Initial conditions: S_1 (blue), S_2 (red).

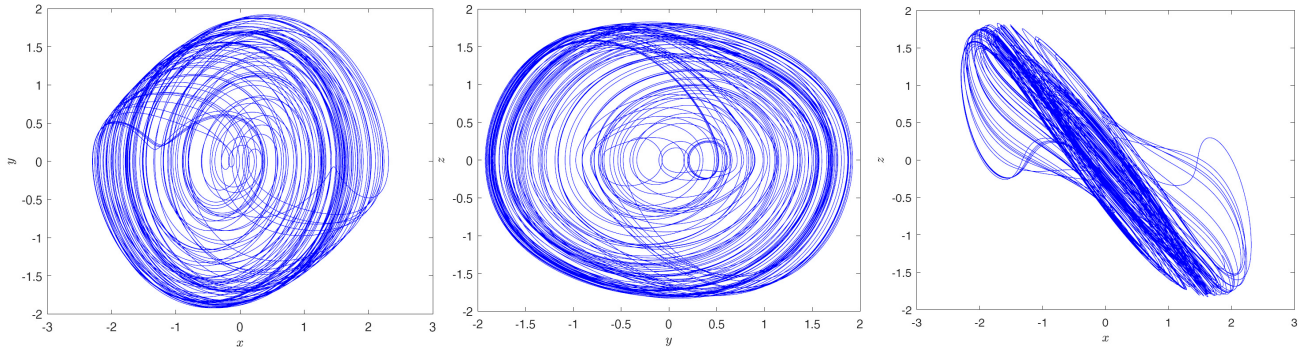

(a) $x - y$ plane **(b)** $y - z$ plane **(c)** $x - z$ plane

Figure 5. 2D views of the chaotic attractor of system (2.5) for $a = 1.67$. Initial conditions: S_1 (blue).

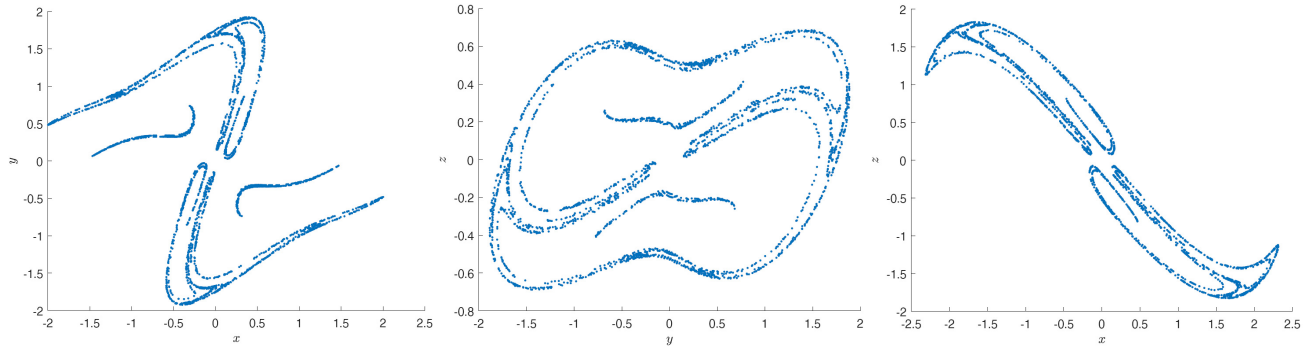

(a) $x - y$ plane **(b)** $y - z$ plane **(c)** $x - z$ plane

Figure 6. Cross-sections of the chaotic attractor of system (2.5) for $a = 1.67$. Initial conditions: S_1 (blue).

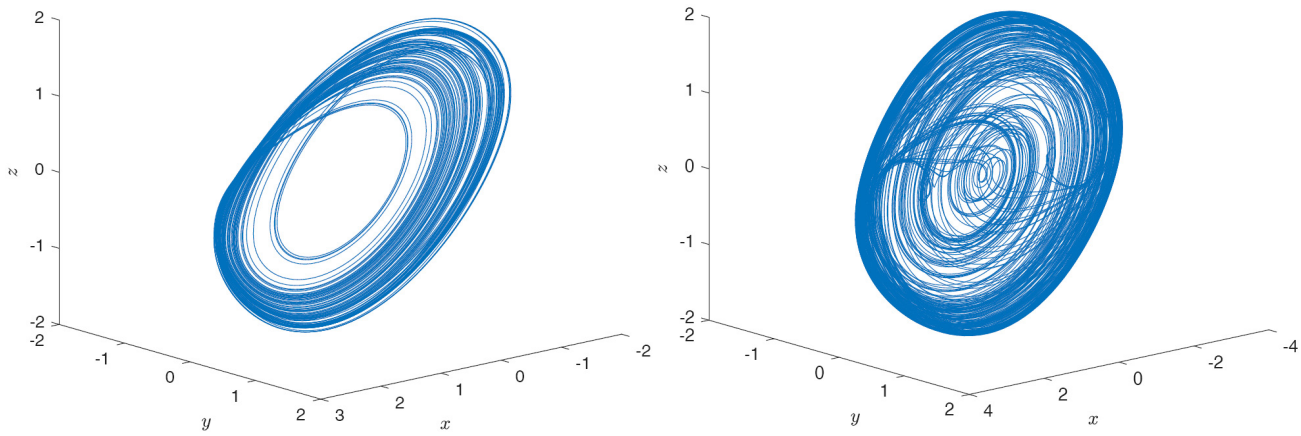

(a) $a = 1.618$ **(b)** $a = 1.67$

Figure 7. Two chaotic attractors of system (2.5). Initial conditions: S_1 (blue).

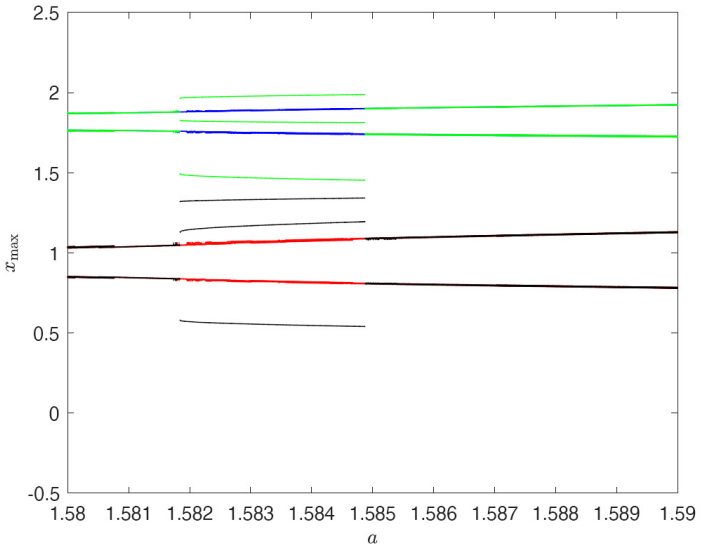

Figure 8. The bifurcation diagram of system (2.5) for $a \in [1.58, 1.59]$.

3.2. Case C

Let us consider system (2.8), which is denoted as Case C. It is obtained from system (2.5) by adding a small constant term 0.01 in the jerk function. In comparison to system (2.5), it is natural for system (2.8) to have some similar dynamical properties, such as the chaotic mechanism and multistability. For more details, please see Figure 9.

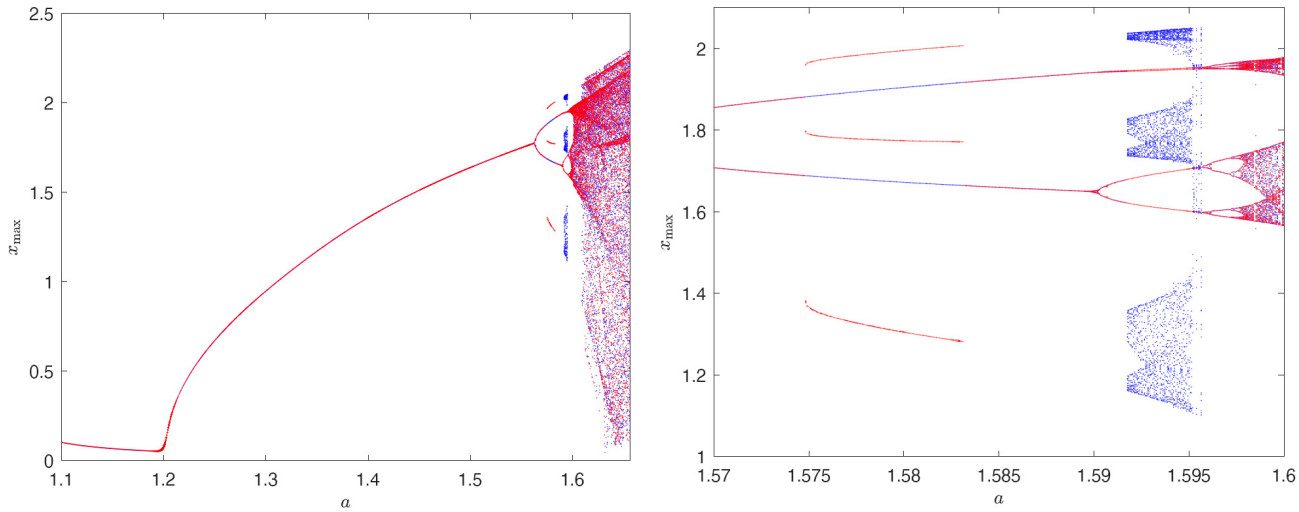

(a) **(b)**

Figure 9. (a) The bifurcation diagram of system (2.8) for $a \in [1.1, 1.656]$. (b) A portion of the bifurcation diagram for $a \in [1.57, 1.6]$. Initial conditions: S_1 (blue), S_2 (red).

With the initial conditions S_3–S_6 and $a \in [1.58, 1.656]$, the bifurcation diagram of system (2.8) is shown in Figure 10. Here, the blue branches correspond to S_3, the red branches correspond to S_4, the green branches correspond to S_5, and the black branches correspond to S_6.

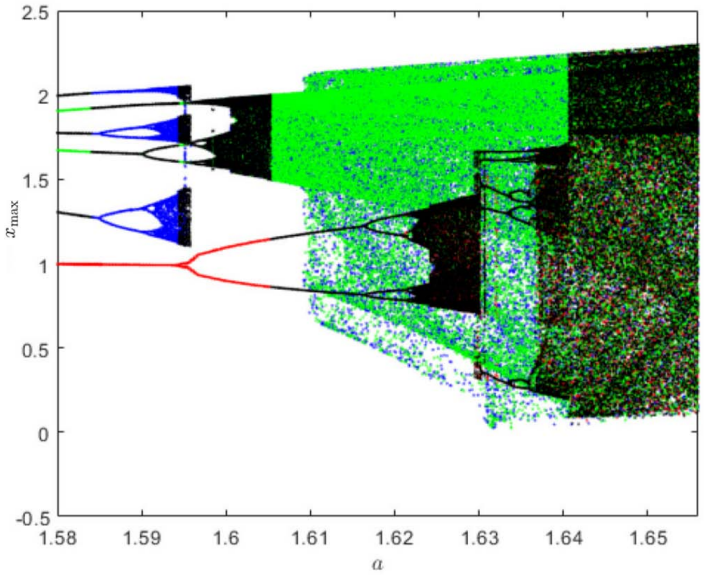

Figure 10. The bifurcation diagram of system (2.8) for $a \in [1.58, 1.656]$.

For $a = 1.58$, period-1 (red), period-2 (green) and period-3 (black) attractors coexist. For $a = 1.627$, two coexisting chaotic attractors (green and black) can be observed.

4. Mechanism II: backward period-doubling route to chaos

This section is about the dynamical analysis and bifurcation analysis of Cases B and D. For these systems, the bifurcation diagrams will be plotted, depicting the local maxima of $x(t)$ versus the parameter a. It would be interesting to see that the underlying mechanisms are the same: backward period-doubling routes to chaos.

The set of six initial conditions are still selected as candidates: $S_i : (x, y, z) = (0, 0, m_i), \quad 1 \le i \le 6$, where

$$m_{1,2} = \pm 0.1, \quad m_{3,4} = \pm 1, \quad m_{5,6} = \pm 0.8. \tag{4.1}$$

4.1. Case B

The bifurcation diagram of system (2.6) is plotted in Figure 11, which depicts the local maxima of $x(t)$ with respect to the parameter a. Here, the two initial conditions are $S_{1,2} : (x, y, z) = (0, 0, \pm 0.1)$. The blue curves correspond to S_1, while red ones correspond to S_2.

Due to Z_2 symmetry, we only describe the long term behaviors of the trajectory starting from the point S_1, corresponding to the blue branches in Figure 11. From the bifurcation diagram, we can see that the system can exhibit a point attractor ($-1.09 \le a \le -0.83$), a pitchfork bifurcation (occurs at the origin when $a = -1$), supercritical Hopf bifurcations (occur at the two nontrivial equilibria for

$a \approx -1.1$), periodic attractors ($-1.33 < a < -1.11$) and a backward period-doubling cascade from chaotic to periodic dynamics. These observations are in good agreement with the Lyapunov exponent spectrum in Figure 12.

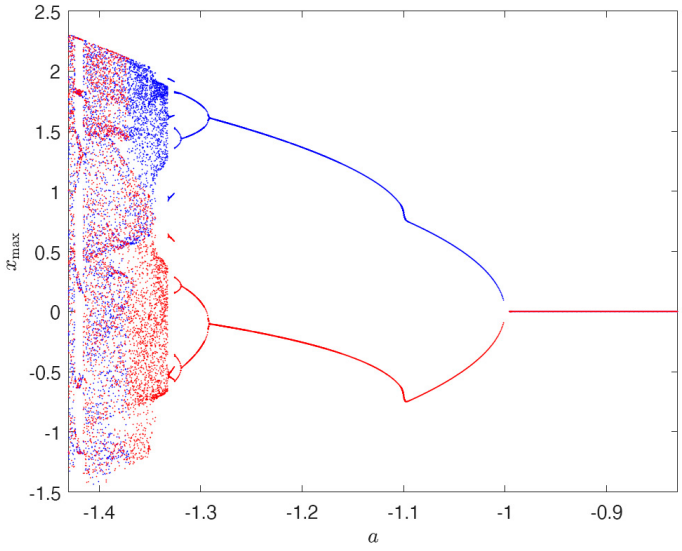

Figure 11. The bifurcation diagram of system (2.6) for $a \in [-1.43, -0.83]$.

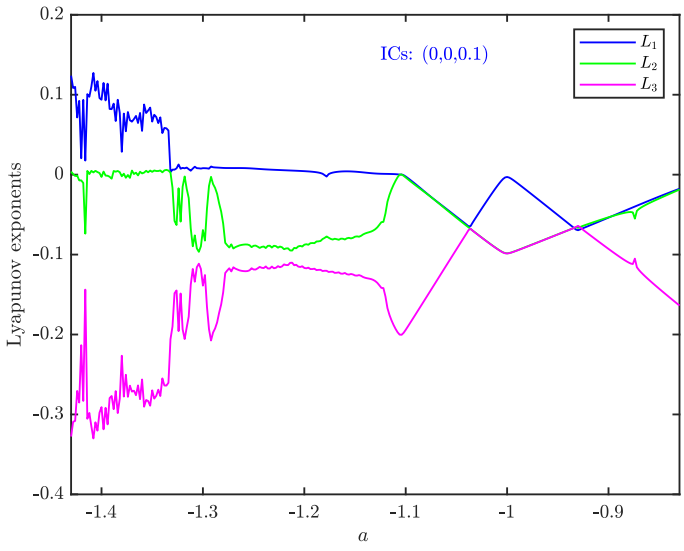

Figure 12. Lyapunov exponent spectrum of system (2.6) for $a \in [-1.43, -0.83]$.

For more details about the local bifurcations, see Section 5. In the following simulations, the blue trajectories correspond to S_1, while the red ones correspond to S_2.

For $a = -1.200, -1.300, -1.325$, the 2D views of coexisting periodic attractors are shown in Figure 13.

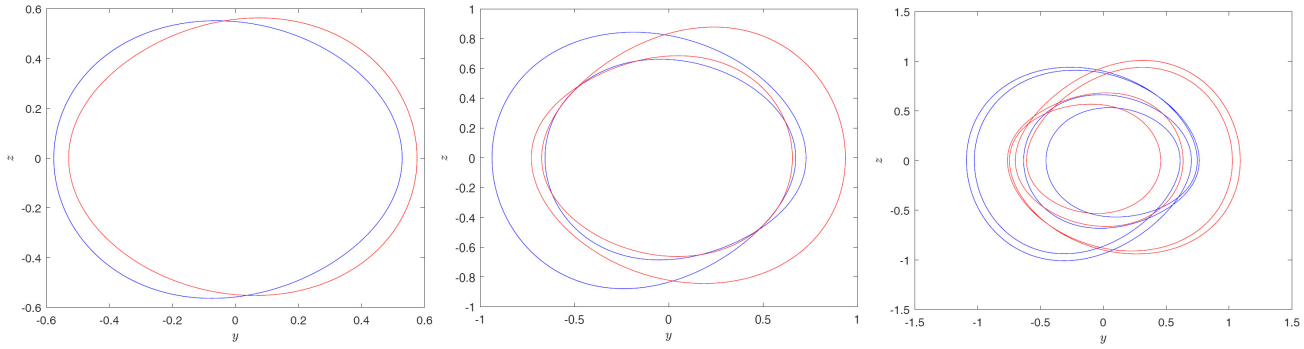

(a) $a = -1.200$ **(b)** $a = -1.300$ **(c)** $a = -1.325$

Figure 13. Coexisting periodic attractors of system (2.6) for $a = -1.200, -1.300$ and -1.325.

For $a = -1.34$, the 2D views of the coexisting chaotic attractors are shown in Figure 14.

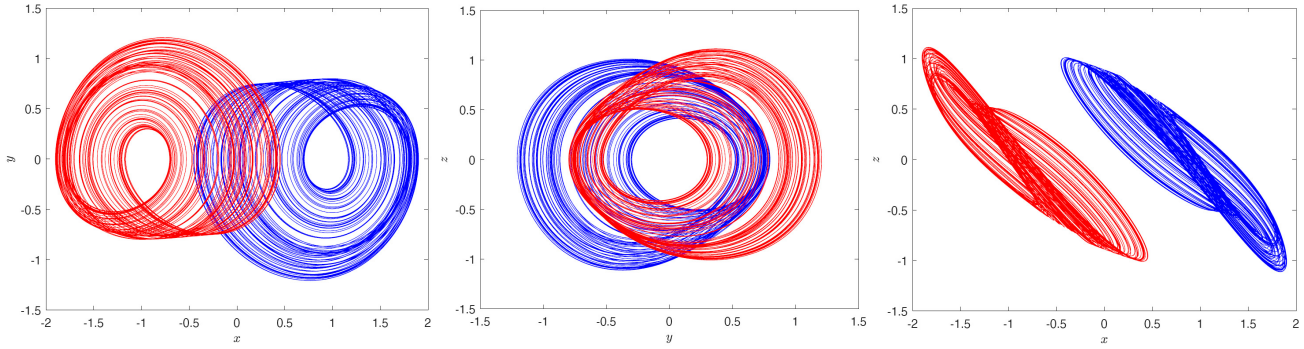

(a) $x - y$ plane **(b)** $y - z$ plane **(c)** $x - z$ plane

Figure 14. 2D views of coexisting chaotic attractors of system (2.6) for $a = -1.34$.

A typical chaotic attractor can be found at $a = -1.4$, which is shown in Figure 15.

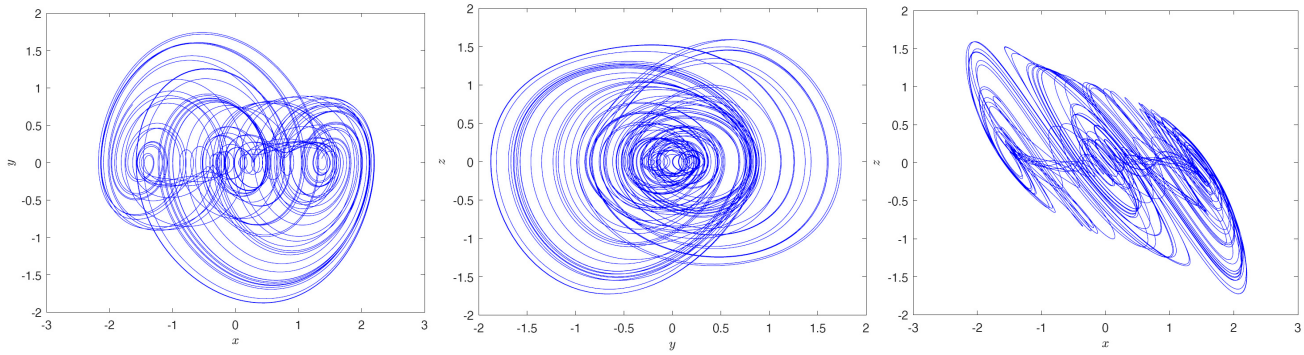

(a) $x - y$ plane **(b)** $y - z$ plane **(c)** $x - z$ plane

Figure 15. 2D views of the chaotic attractor of system (2.6) for $a = -1.4$.

To illustrate the folding and stretching structure of the attractor, cross-sections (two-side Poincaré sections) are plotted in Figure 16. Further analysis shows that a boundary crisis occurs at $a = -1.433$.

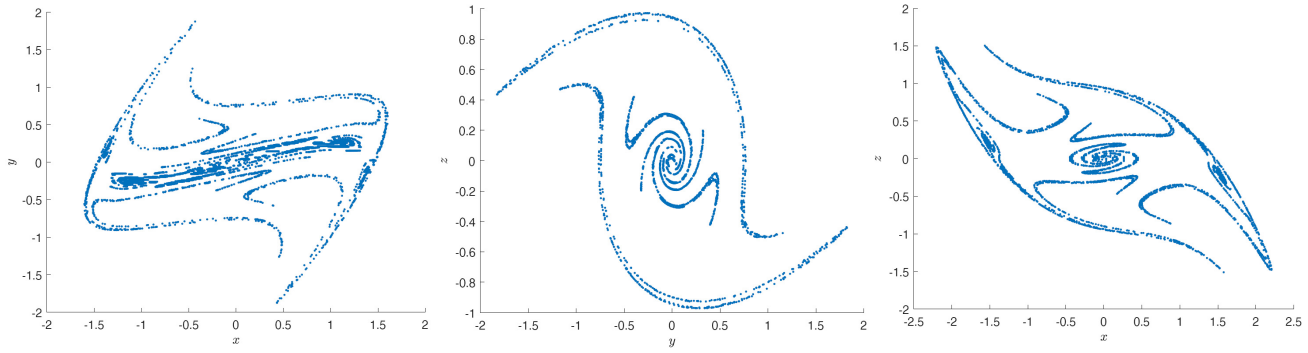

(a) $x - y$ plane **(b)** $y - z$ plane **(c)** $x - z$ plane

Figure 16. Cross-sections of the chaotic attractor of system (2.6) for $a = -1.4$.

The 3D attractors of the system for $a = -1.34$, $a = -1.4$ are plotted in Figure 17, which are one-scroll and two-scroll chaotic attractors, respectively.

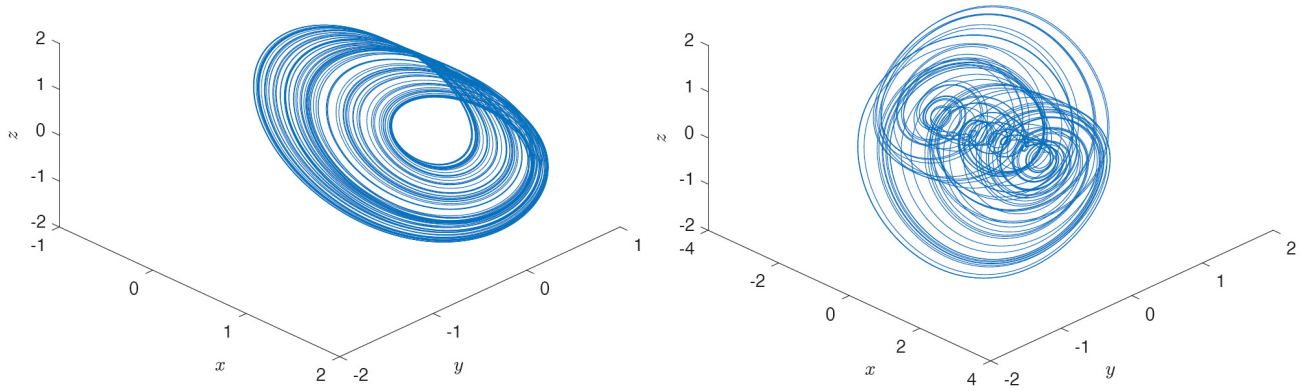

(a) $a = -1.34$ **(b)** $a = -1.4$

Figure 17. Chaotic attractors of system (2.6) for $a = -1.34$ and $a = -1.4$.

For the latter chaotic attractor, the Lyapunov exponents are 0.1042, 0, −0.3042, and thus the Kaplan-Yorke dimension is $D_{\mathrm{KY}} = 2.3425$.

4.2. Case D

Let us consider the system (2.9), which is denoted as Case D. It is obtained from system (2.6) by adding a small constant term 0.01 in the jerk function. In comparison to system (2.6), it is natural for system (2.9) to have some similar dynamical properties, such as the chaotic mechanism and multistability. Using the two initial conditions S_1 and S_2, the bifurcation diagram of system (2.9) is shown in Figure 18. The bifurcation diagram of system (2.9) is also shown in Figure 19, in which the four initial conditions S_3–S_6 are used. In Figure 19, there is a quite narrow range near $a = -1.33$ corresponding to two coexisting period four attractors and one chaotic attractor. For $a = -1.29$, the phase portrait of two coexisting asymmetric periodic attractors is shown in Figure 20. For $a = -1.35$, the phase portrait of two coexisting asymmetric chaotic attractors is shown in Figure 21.

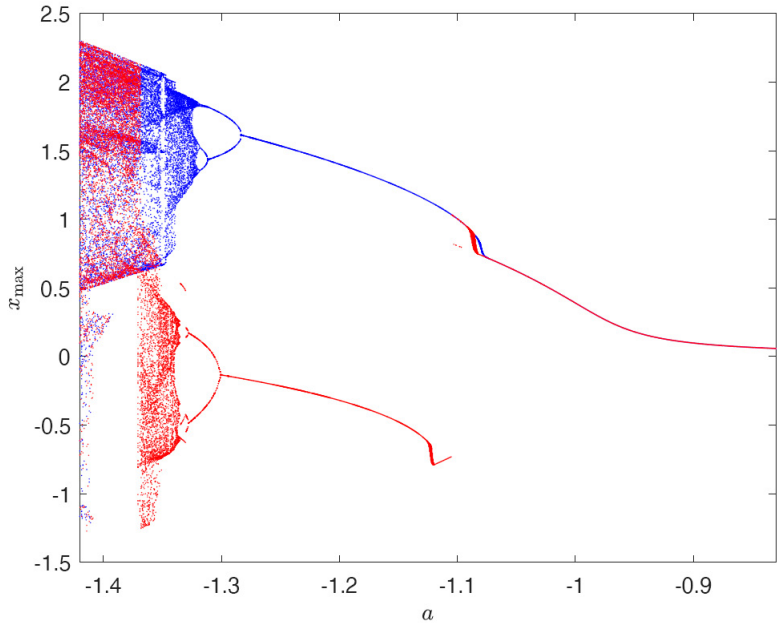

Figure 18. The bifurcation diagram of system (2.9) for $a \in [-1.42, -0.83]$. Initial conditions: S_1 (blue), S_2 (red).

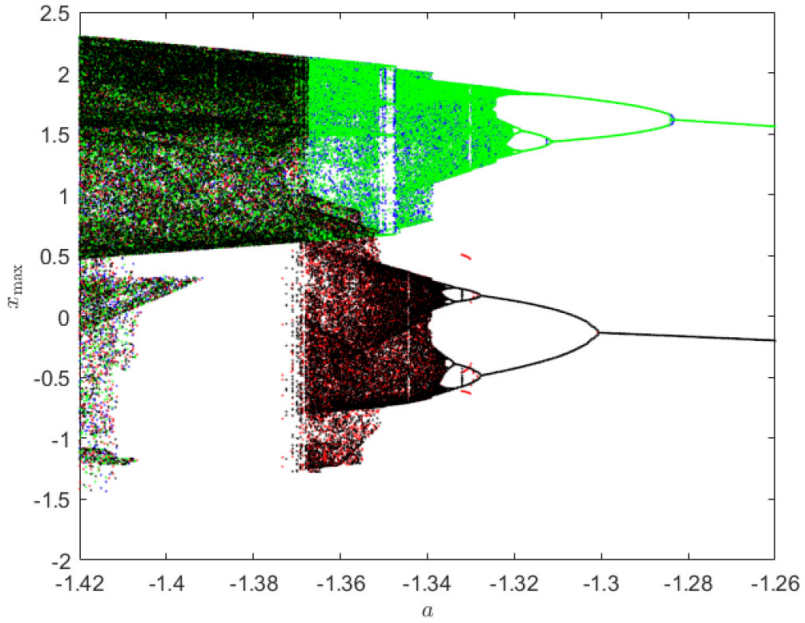

Figure 19. The bifurcation diagram of system (2.9) for $a \in [-1.42, -1.26]$. Initial conditions: S_3 (blue), S_4 (red), S_5 (green), S_6 (black).

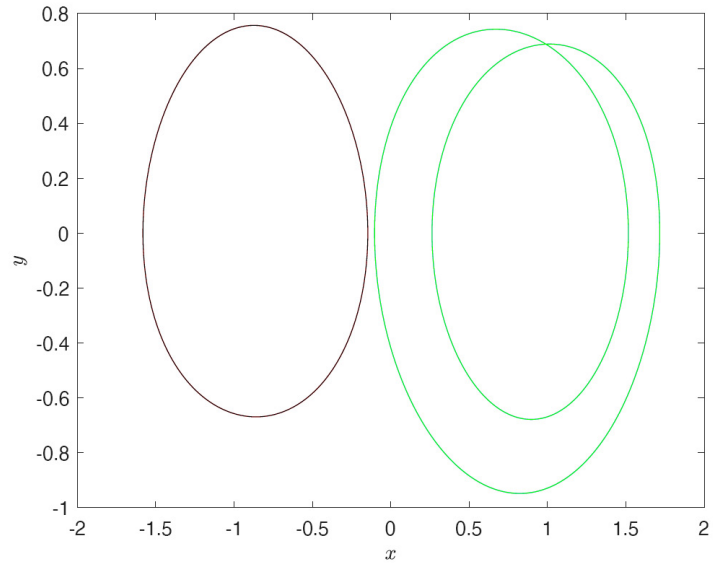

Figure 20. Two coexisting periodic attractors of system (2.9) for $a = -1.29$. Initial conditions: S_5 (green), S_6 (black).

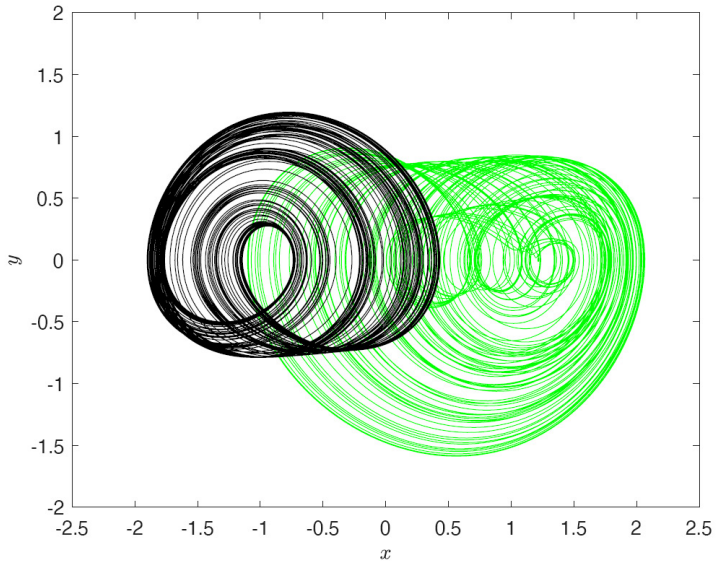

Figure 21. Two coexisting chaotic attractors of system (2.9) for $a = -1.35$. Initial conditions: S_5 (green), S_6 (black).

5. Local bifurcation analysis

It is very known that both pitchfork bifurcation and Hopf bifurcation occur in the Lorenz system. These bifurcations and homoclinic bifurcation play important roles in locating chaotic dynamics. It is very interesting to see that both pitchfork bifurcation and Hopf bifurcation are also available in the jerk

system (2.3), including both subcritical and supercritical versions. These two bifurcations can help us understand the mechanisms of chaotic attractors presented in Sections 3 and 4.

5.1. Pitchfork bifurcation at the origin for $a = d$

The following lemma is due to Sotomayor [57,58] and is the standard tool for proving the existence of a pitchfork bifurcation. Consider the following system:

$$\frac{dx}{dt} = g(x, \mu), \qquad x \in \mathbb{R}^n, \ \mu \in \mathbb{R}, \tag{5.1}$$

where g is sufficiently smooth, and μ is a parameter. As usual, $Dg(x, \mu)$ denotes the Jacobian matrix of the function g with respect to the variable x, and $g_\mu(x, \mu)$ represents the partial derivative of g with respect to μ.

Lemma 5.1. *Consider the system* (5.1). *When $\mu = \mu_0$, assume that there is an equilibrium x_0, for which the following hypotheses are satisfied:*

(i) The Jacobian matrix $Dg(x_0, \mu_0)$ has a simple eigenvalue 0 with right eigenvector v and left eigenvector w. It also has k eigenvalues with negative real part and $n - k - 1$ eigenvalues with positive real part.

(ii) $w^T g_\mu(x_0, \mu_0) = 0$.

(iii) $w^T [D^2 g(x_0, \mu_0)(v, v)] = 0$.

(iv) $w^T [Dg_\mu(x_0, \mu_0)v] \neq 0$.

(v) $w^T [D^3 g(x_0, \mu_0)(v, v, v)] \neq 0$.

Then, the system experiences a pitchfork bifurcation at the equilibrium x_0 as the parameter μ passes through $\mu = \mu_0$.

Let us return to system (2.3), which always has a trivial equilibrium located at the origin. For $\frac{a}{d} > 1$, it also has a pair of symmetric equilibria $P_{1,2} = (\pm x_0, 0, 0)$, where

$$\frac{\sinh(x_0)}{x_0} = \frac{a}{d}.$$

For $\frac{a}{d} \leq 1$, there is no other equilibrium except the origin.

The Jacobian matrix of the system at the origin is

$$J(a) = \begin{bmatrix} 0 & 1 & 0 \\ 0 & 0 & 1 \\ d - a & -b^2 & -c \end{bmatrix}, \tag{5.2}$$

whose characteristic equation is

$$h(\lambda, a) = \lambda^3 + c\lambda^2 + b^2\lambda + (a - d) = 0. \tag{5.3}$$

Theorem 5.1. *Assume that the conditions* (2.4) *hold. If* $a \in (d, d + cb^2)$*, then the origin is an asymptotically stable equilibrium of system* (2.3)*.*

Proof. According to the Routh-Hurwitz criterion and the assumption (2.4), all the eigenvalues of $J(a)$ have negative real parts if and only if $d < a < d + cb^2$. Thus, the conclusion follows. □

Theorem 5.2. *For system* (2.3)*, a pitchfork bifurcation occurs at the origin as a passes through* $a = d$*. Moreover, if* $d < 0$*, the bifurcation is supercritical, while if* $d > 0$*, it is subcritical.*

Proof. Take a as the bifurcation parameter. Let $f(\mathrm{x}, a)$ be the vector field of system (2.3) with $\mathrm{x} = (x, y, z)$.

When $a = d$, the origin is the unique equilibrium of the system. In this case, the Jacobian matrix of f at this point is

$$J(d) = \begin{bmatrix} 0 & 1 & 0 \\ 0 & 0 & 1 \\ 0 & -b^2 & -c \end{bmatrix}. \tag{5.4}$$

It has a simple eigenvalue 0 with a right eigenvector

$$v = (1, 0, 0)^T$$

and a left eigenvector

$$w = (b^2, c, 1)^T.$$

A direct computation gives

$$\begin{aligned} w^T f_a(0, d) &= 0, \\ w^T [D^2 f(0, d)(v, v)] &= 0, \\ w^T [D f_a(0, d) v] &= -1, \\ w^T [D^3 f(0, d)(v, v, v)] &= d. \end{aligned}$$

According to Lemma 5.1, a pitchfork bifurcation occurs at the origin for $a = d$. Furthermore, according to [57], this bifurcation is supercritical if $d < 0$, while it is subcritical if $d > 0$. □

5.2. Hopf bifurcation at the origin for $a = d + cb^2$

It is well known that Hopf bifurcation is a typical phenomenon related to the appearance or disappearance of limit cycles. It can be studied through some characteristic quantities, such as bifurcation formulas [59], Lyapunov coefficients [60] and focus quantities [61, 62]. For system (2.3), in order to obtain the direction of bifurcation and the period, amplitude, stability of limit cycles, we use the method of Hassard et al. [59] to get the results.

Before we state the results, let us introduce a notation:

$$a_0 = d + cb^2. \tag{5.5}$$

Theorem 5.3. *Assume that the conditions* (2.4) *hold. Then, for system* (2.3)*, the following statements hold:*

(i) A Hopf bifurcation occurs at the origin as a passes through $a = a_0$.

(ii) If $d > 0$, the Hopf bifurcation is supercritical, leading to a family of stable limit cycles for $a > a_0$ and $a - a_0$ being sufficiently small.

(iii) If $d < 0$, the Hopf bifurcation is subcritical, leading to a family of unstable limit cycles for $a < a_0$ and $a_0 - a$ being sufficiently small.

(iv) The period of the limit cycle can be expanded in the form

$$T(a) = \frac{2\pi}{b} + O(|a - a_0|^2).$$

(v) The limit cycles are approximated by

$$\begin{cases} x(t) = A\cos(bt) + O(|a - a_0|^2), \\ y(t) = -Ab\sin(bt) + O(|a - a_0|^2), \\ z(t) = -Ab^2\cos(bt) + O(|a - a_0|^2), \end{cases} \tag{5.6}$$

where $A = \sqrt{\dfrac{8(a - a_0)}{d}}$.

Proof. In view of (5.2) and (5.3), according to the Proposition in [63], a Hopf bifurcation may occur at the origin when a passes through $a = a_0$. When $a = a_0$, the eigenvalues of the Jacobian matrix at the origin are $\lambda_{1,2} = \pm b\mathrm{i}$, $\lambda_3 = -c$.

In order to prove (i), it suffices to verify the transversality condition. From (5.3), we have

$$\begin{aligned} \lambda_1'(a_0) &= -\frac{h_a}{h_\lambda}\Big|_{a=a_0,\lambda=b\mathrm{i}} \\ &= \frac{1}{2(b^2 + c^2)} + \frac{c}{2b(b^2 + c^2)}\mathrm{i}. \end{aligned} \tag{5.7}$$

Let

$$\lambda_1'(a_0) := \alpha'(0) + \omega'(0)\mathrm{i}. \tag{5.8}$$

By the assumption (2.4), we have

$$\alpha'(0) = \frac{1}{2(b^2 + c^2)} > 0, \qquad \omega'(0) = \frac{c}{2b(b^2 + c^2)} > 0,$$

indicating that the transversality condition is satisfied. Hence, the statement (i) holds.

The other statements are based on the computation of μ_2, τ_2 and β_2 [59]. Setting $a = a_0$ and using the transformation

$$\begin{cases} x = y_1 + y_3, \\ y = -by_2 - cy_3, \\ z = -b^2y_1 + c^2y_3, \end{cases}$$

system (2.3) becomes

$$\begin{cases} \dfrac{dy_1}{dt} = -by_2 - \dfrac{dy_1^3}{6(b^2+c^2)} - \dfrac{dy_3y_1^2}{2(b^2+c^2)} - \dfrac{dy_3^2y_1}{2(b^2+c^2)} - \dfrac{dy_3^3}{6(b^2+c^2)} + O(5), \\ \dfrac{dy}{dt} = by_1 - \dfrac{cdy_1^3}{6b(b^2+c^2)} - \dfrac{cdy_3y_1^2}{2b(b^2+c^2)} - \dfrac{cdy_3^2y_1}{2b(b^2+c^2)} - \dfrac{cdy_3^3}{6b(b^2+c^2)} + O(5), \\ \dfrac{dz}{dt} = -cy_3 + \dfrac{dy_1^3}{6(b^2+c^2)} + \dfrac{dy_3y_1^2}{2(b^2+c^2)} + \dfrac{dy_3^2y_1}{2(b^2+c^2)} + \dfrac{dy_3^3}{6(b^2+c^2)} + O(5). \end{cases}$$

Now, we are in the position for applying the algorithm of Hassard et al. [59]. Using the same notation as in [59], by computation we have

$$\begin{gathered} g_{11} = g_{02} = g_{20} = G_{110} = G_{101} = 0, \\ g_{21} = G_{21},\ c_1(0) = \frac{g_{21}}{2}, \\ \mu_2 = -\frac{\operatorname{Re} c_1(0)}{\alpha'(0)}, \\ \tau_2 = -\frac{\operatorname{Im} c_1(0) + \mu_2\omega'(0)}{\omega_0}, \\ \beta_2 = 2\ \operatorname{Re} c_1(0), \end{gathered}$$

where

$$\omega_0 = b, \qquad G_{2,1} = -\frac{d}{8(b^2+c^2)} - \frac{cd}{8b(b^2+c^2)}\mathrm{i}.$$

Therefore, we have

$$\mu_2 = \frac{d}{8},\ \ \tau_2 = 0,\ \ \beta_2 = -\frac{d}{8(b^2+c^2)}.$$

Based on these three quantities and Hopf bifurcation theory [59], the conclusions (ii)–(v) hold. □

6. PSIM simulations

PSIM (power simulation) is one of the fastest simulators for power electronics simulations. We use PSIM circuit simulation to validate the chaotic behavior of the following system:

$$\begin{cases} \dfrac{dx}{dt} = y, \\ \dfrac{dy}{dt} = z, \\ \dfrac{dz}{dt} = -1.67\,x - y - 0.2\,z + \sinh(x), \end{cases} \tag{6.1}$$

for which the numerical chaotic attractor was shown in Figure 5.

The circuit model of the system is shown in Figure 22. It has three operational channels, three integrators, two inverters and one hyperbolic sine converter. More specifically, the model has ten resistors with the following values:

$$R_1 = R_2 = R_4 = R_6 = R/1 = 10\ \mathrm{k}\Omega,$$

$$R_3 = R/1.67 = 5.988\ \text{k}\Omega,\ R_5 = R/0.2 = 50\ \text{k}\Omega,$$
$$R_{a1} = R_{a2} = R_{b1} = R_{b2} = 10\ \text{k}\Omega.$$

It also has three capacitors with the values $C_1 = C_2 = C_3 = C = 100$ nF. All power supplies of the operational amplifiers (op-amps) are ±15 V.

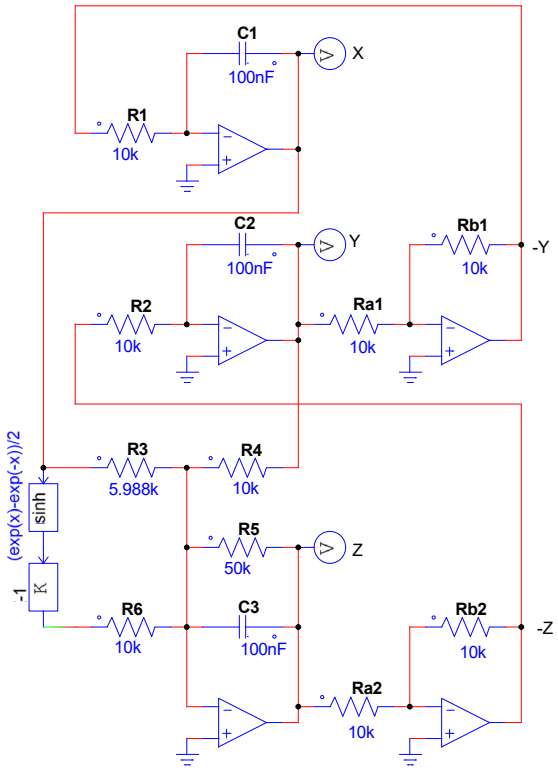

Figure 22. Analog circuit implementation of system (6.1).

Let X, Y, Z be the output voltages of capacitors C_1, C_2 and C_3, respectively. By applying Kirchhoff's circuit laws to the circuit model, the state equations for X, Y, Z are described by

$$\begin{cases} \dfrac{dX}{dt} = \dfrac{1}{RC}\left(\dfrac{R}{R_1}Y\right), \\ \dfrac{dY}{dt} = \dfrac{1}{RC}\left(\dfrac{R}{R_2}Z\right), \\ \dfrac{dZ}{dt} = \dfrac{1}{RC}\left(-\dfrac{R}{R_3}X - \dfrac{R}{R_4}Y - \dfrac{R}{R_5}Z + \dfrac{R}{R_6}\sinh(X)\right). \end{cases} \tag{6.2}$$

The initial values used for the simulations are $X(0) = Y(0) = 0$ V, $Z(0) = 0.1$ V. Using PSIM 9.0.3, the phase portraits of the chaotic attractor are simulated and are shown in Figure 23. The results show that the circuit simulations are consistent with the results of numerical ones in Figure 5.

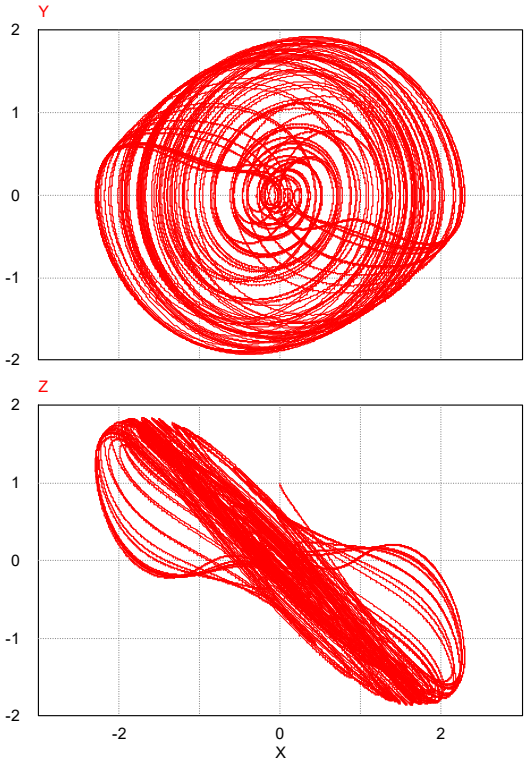

Figure 23. The simulated chaotic attractor of system (6.2) .

7. Conclusions

Jerk systems are very attractive due to simple forms and rich dynamical behaviors. More importantly, such systems can be realized with compact electrical circuit structures. In this paper, a jerk system with a hyperbolic sine nonlinearity and five parameters is proposed and explored. For the case with $\varepsilon = 0$, the jerk system displays very rich local bifurcation structures, which are rigorously treated in Section 5. Such local bifurcations are important for the analysis of the transitions from simple to complex dynamics in the general jerk systems. The novelty of this paper lies in the discovery of mechanisms leading to chaotic attractors in four jerk systems. Simultaneously, the corresponding multistability problems are also discussed. Two mechanisms with different bifurcation processes are investigated in detail for the four systems. In the first mechanism, the continuation of a pitchfork bifurcation (which is followed by a Hopf bifurcation) gives rise to forward period doubling cascades to chaos. In the second mechanism, the continuation of a pitchfork bifurcation (which is followed by a Hopf bifurcation) gives rise to backward period doubling cascades to chaos. In fact, the numerical findings in this paper rely on some very basic local bifurcations of the origin, which are rigorously treated in Section 5. In general, local bifurcations are of great importance for understanding the complex phenomena of chaotic mechanisms and multistabilities. Using PSIM, the circuit implementation is carried out, which verifies the chaotic response of a jerk system through simulations. For future studies, we hope the jerk circuit model in this paper can be used in secure communications, electronic circuits, random number generators and image encryption.

Acknowledgments

This research was funded by Shandong Provincial Natural Science Foundation, China (ZR2018MA025).

Conflict of interest

The authors declare that they have no competing interests in this paper.

References

1. A. Jones, N. Strigul, Is spread of COVID-19 a chaotic epidemic? *Chaos Solitons Fract.*, **142** (2021), 110376. https://doi.org/10.1016/j.chaos.2020.110376
2. H. Iro, *A modern approach to cassical mechanics*, Singarpore: World Scientific, 2015. https://doi.org/10.1142/9655
3. A. T. Johnson, *Biology for engineers*, Boca Raton, Florida: CRC Press, 2018. https://doi.org/10.1201/9781351165648
4. K. H. Sun, *Chaotic secure communication: Principles and technologies*, Beijing: Tsinghua University Press, 2016.
5. E. N. Lorenz, Deterministic nonperiodic flow, *J. Atmos. Sci.*, **20** (1963), 130–141.
6. O. E. Rössler, An equation for continuous chaos, *Phys. Lett. A*, **57** (1976), 397–398. https://doi.org/10.1016/0375-9601(76)90101-8
7. G. R. Chen, T. Ueta, Yet another chaotic attractor, *Int. J. Bifurcat. Chaos*, **9** (1999), 1465–1466. https://doi.org/10.1142/S0218127499001024
8. Q. G. Yang, Z. C. Wei, G. R. Chen, An unusual 3D autonomous quadratic chaotic system with two stable node-foci, *Int. J. Bifurcat. Chaos*, **20** (2010), 1061–1083. https://doi.org/10.1142/S0218127410026320
9. J. C. Sprott, *Elegant chaos: Algebraically simple chaotic flows*, Singapore: World Scientific, 2010.
10. J. C. Sprott, Strange attractors with various equilibrium types, *Eur. Phys. J. Spec. Top.*, **224** (2015), 1409–1419. https://doi.org/10.1140/epjst/e2015-02469-8
11. Z. Wang, Z. C. Wei, K. H. Sun, S. B. He, H. H. Wang, Q. Xu, et al., Chaotic flows with special equilibria, *Eur. Phys. J. Spec. Top.*, **229** (2020), 905–919. https://doi.org/10.1140/epjst/e2020-900239-2
12. G. A. Leonov, N. V. Kuznetsov, Hidden attractors in dynamical systems. From hidden oscillations in Hilbert-Kolmogorov, Aizerman, and Kalman problems to hidden chaotic attractor in Chua circuits, *Int. J. Bifurcat. Chaos*, **23** (2013), 1330002. https://doi.org/10.1142/S0218127413300024
13. S. N. Chowdhurry, D. Ghosh, Hidden attractors: A new chaotic system without equilibria, *Eur. Phys. J. Spec. Top.*, **229** (2020), 1299–1308. https://doi.org/10.1140/epjst/e2020-900166-7
14. X. Wang, A. Akgul, S. Cicek, V. T. Pham, D. V. Hoang, A chaotic system with two stable equilibrium points: Dynamics, circuit realization and communication application, *Int. J. Bifurcat. Chaos*, **27** (2017), 1750130. https://doi.org/10.1142/S0218127417501309

15. S. Jafari, J. C. Sprott, V. T. Pham, C. Volos, C. B. Li, Simple chaotic 3D flows with surfaces of equilibria, *Nonlinear Dyn.*, **86** (2016), 1349–1358. https://doi.org/10.1007/s11071-016-2968-x
16. S. T. Kingni, V. T. Pham, S. Jafari, P. Woafo, A chaotic system with an infinite number of equilibrium points located on a line and on a hyperbola and its fractional-order form, *Chaos Solitons Fract.*, **99** (2017), 209–218. https://doi.org/10.1016/j.chaos.2017.04.011
17. Y. J. Dong, G. Y. Wang, H. H. Iu, G. R. Chen, L. Chen, Coexisting hidden and self-excited attractors in a locally active memristor-based circuit, *Chaos*, **30** (2020), 103123. https://doi.org/10.1063/5.0002061
18. T. Kapitaniak, G. A. Leonov, Multistability: Uncovering hidden attractors, *Eur. Phys. J. Spec. Top.*, **224** (2015), 1405–1408. https://doi.org/10.1140/epjst/e2015-02468-9
19. N. Wang, G. S. Zhang, N. V. Kuznetsov, H. Bao, Hidden attractors and multistability in a modified Chua's circuit, *Commun. Nonlinear Sci. Numer. Simul.*, **92** (2021), 105494. https://doi.org/10.1016/j.cnsns.2020.105494
20. X. Wang, N. V. Kuznetsov, G. R. Chen, *Chaotic systems with multistability and hidden attractors*, New York: Springer, 2021. https://doi.org/10.1007/978-3-030-75821-9
21. M. N. Zavareh, F. Nazarimehr, K. Rajagopal, S. Jafari, Hidden attractor in a passive motion model of compass-gait robot, *Int. J. Bifurcat. Chaos*, **28** (2018), 1850171. https://doi.org/10.1142/S0218127418501717
22. A. Prasad, Existence of perpetual points in nonlinear dynamical systems and its applications, *Int. J. Bifurcat. Chaos*, **25** (2015), 1530005. https://doi.org/10.1142/S0218127415300050
23. D. Dudkowski, A. Prasad, T. Kapitaniak, Perpetual points and hidden attractors in dynamical systems, *Phys. Lett. A*, **379** (2015), 2591–2596. https://doi.org/10.1016/j.physleta.2015.06.002
24. F. Nazarimehr, B. Saedi, S. Jafari, J. C. Sprott, Are perpetual points sufficient for locating hidden attractors? *Int. J. Bifurcat. Chaos*, **27** (2017), 1750037. https://doi.org/10.1142/S0218127417500377
25. D. Dudkowski, A. Prasad, T. Kapitaniak, Describing chaotic attractors: Regular and perpetual points, *Chaos*, **28** (2018), 033604. https://doi.org/10.1063/1.4991801
26. A. K. Farhan, N. M. G. Al-Saidi, A. T. Maolood, F. Nazarimehr, I. Hussain, Entropy analysis and image encryption application based on a new chaotic system crossing a cylinder, *Entropy*, **21** (2019), 1–14. https://doi.org/10.3390/e21100958
27. U. Çavuçoğlu, S. Panahi, A. Akgül, S. Jafari, S. Kaçar, A new chaotic system with hidden attractor and its engineering applications: Analog circuit realization and image encryption, *Analog Integr. Circ. Sig. Process*, **98** (2019), 85–99. https://doi.org/10.1007/s10470-018-1252-z
28. A. N. Pisarchik, U. Feudel, Control of multistability, *Phys. Rep.*, **540** (2014), 167–218. https://doi.org/10.1016/j.physrep.2014.02.007
29. S. Morfu, B. Nofiele, P. Marquié, On the use of multistability for image processing, *Phys. Lett. A*, **367** (2007), 192–198. https://doi.org/10.1016/j.physleta.2007.02.086
30. Z. T. Njitacke, S. D. Isaac, T. Nestor, J. Kengne, Window of multistability and its control in a simple 3D Hopfield neural network: Application to biomedical image encryption, *Neural Comput. Appl.*, **33** (2021), 6733–6752. https://doi.org/10.1007/s00521-020-05451-z
31. M. Lines, *Nonlinear dynamical systems in economics*, CISM, Vol. 476, Vienna: Springer, 2005. https://doi.org/10.1007/3-211-38043-4

32. B. Chen, X. X. Cheng, H. Bao, M. Chen, Q. Xu, Extreme multistability and its incremental integral reconstruction in a non-autonomous memcapacitive oscillator, *Mathematics*, **10** (2022), 1–13. https://doi.org/10.3390/math10050754
33. J. C. Sprott, S. Jafari, A. J. M. Khalaf, T. Kapitaniak, Megastability: Coexistence of a countable infinity of nested attractors in a periodically-forced oscillator with spatially-periodic damping, *Eur. Phys. J. Spec. Top.*, **226** (2017), 1979–1985. https://doi.org/10.1140/epjst/e2017-70037-1
34. V. Patidar, K. K. Sud, Bifurcation and chaos in simple jerk dynamical systems, *Pramana*, **64** (2005), 75–93. https://doi.org/10.1007/BF02704532
35. G. Innocenti, A. Tesi, R. Genesio, Complex behavior analysis in quadratic jerk systems via frequency domain Hopf bifurcation, *Int. J. Bifurcat. Chaos*, **20** (2010), 657–667. https://doi.org/10.1142/S0218127410025946
36. B. Sang, B. Huang, Zero-Hopf bifurcations of 3D quadratic jerk system, *Mathematics*, **8** (2020), 1–19. https://doi.org/10.3390/math8091454
37. Z. C. Wei, J. C. Sprott, H. Chen, Elementary quadratic chaotic flows with a single non-hyperbolic equilibrium, *Phys. Lett. A*, **379** (2015), 2184–2187. https://doi.org/10.1016/j.physleta.2015.06.040
38. K. E. Chlouverakis, J. C. Sprott, Chaotic hyperjerk systems, *Chaos Solitons Fract.*, **28** (2006), 739–746. https://doi.org/10.1016/j.chaos.2005.08.019
39. F. Y. Dalkiran, J. C. Sprott, Simple chaotic hyperjerk system, *Int. J. Bifurcat. Chaos*, **26** (2016), 1650189. https://doi.org/10.1142/S0218127416501893
40. J. P. Singh, V. T. Pham, T. Hayat, S. Jafari, F. E. Alsaadi, B. K. Roy, A new four-dimensional hyperjerk system with stable equilibrium point, circuit implementation, and its synchronization by using an adaptive integrator backstepping control, *Chinese Phys. B*, **27** (2018), 100501. https://doi.org/10.1088/1674-1056/27/10/100501
41. G. D. Leutcho, J. Kengne, L. K. Kengne, Dynamical analysis of a novel autonomous 4-D hyperjerk circuit with hyperbolic sine nonlinearity: Chaos, antimonotonicity and a plethora of coexisting attractors, *Chaos Solitons Fract.*, **107** (2018), 67–87. https://doi.org/10.1016/j.chaos.2017.12.008
42. I. Ahmad, B. Srisuchinwong, W. San-Um, On the first hyperchaotic hyperjerk system with no equilibria: A simple circuit for hidden attractors, *IEEE Access*, **6** (2018), 35449–35456. https://doi.org/10.1109/ACCESS.2018.2850371
43. P. Ketthong, B. Srisuchinwong, A damping-tunable snap system: From dissipative hyperchaos to conservative chaos, *Entropy*, **24** (2022), 1–14. https://doi.org/10.3390/e24010121
44. M. Joshi, A. Ranjan, An autonomous simple chaotic jerk system with stable and unstable equilibria using reverse sine hyperbolic functions, *Int. J. Bifurcat. Chaos*, **30** (2020), 2050070. https://doi.org/10.1142/S0218127420500704
45. K. Rajagopal, S. T. Kingni, G. F. Kuiate, V. K. Tamba, V. T. Pham, Autonomous jerk oscillator with cosine hyperbolic nonlinearity: Analysis, FPGA implementation, and synchronization, *Adv. Math. Phys.*, **2018** (2018), 1–12. https://doi.org/10.1155/2018/7273531
46. C. Volos, A. Akgul, V. T. Pham, I. Stouboulos, I. Kyprianidis, A simple chaotic circuit with a hyperbolic sine function and its use in a sound encryption scheme, *Nonlinear Dyn.*, **89** (2017), 1047–1061. https://doi.org/10.1007/s11071-017-3499-9
47. J. Kengne, Z. T. Njitacke, A. N. Negou, M. F. Tsostop, H. B. Fotsin, Coexistence of multiple attractors and crisis route to chaos in a novel chaotic jerk circuit, *Int. J. Bifurcat. Chaos*, **26** (2016), 1650081. https://doi.org/10.1142/S0218127416500814

48. L. K. Kengne, J. Kengne, J. R. M. Pone, H. T. K. Tagne, Symmetry breaking, coexisting bubbles, multistability, and its control for a simple jerk system with hyperbolic tangent nonlinearity, *Complexity*, **2020** (2020), 1–24. https://doi.org/10.1155/2020/2340934
49. Y. Li, Y. C. Zeng, J. F. Zeng, A unique jerk system with abundant dynamics: Symmetric or asymmetric bistability, tristability, and coexisting bubbles, *Braz. J. Phys.*, **50** (2020), 153–163. https://doi.org/10.1007/s13538-019-00731-z
50. M. Molaie, S. Jafari, J. C. Sprott, S. M. R. H. Golpayegani, Simple chaotic flows with one stable equilibrium, *Int. J. Bifurcat. Chaos*, **23** (2013), 1350188. https://doi.org/10.1142/S0218127413501885
51. M. Liu, B. Sang, N. Wang, I. Ahmad, Chaotic dynamics by some quadratic jerk systems, *Axioms*, **10** (2021), 1–18. https://doi.org/10.3390/axioms10030227
52. C. B. Li, J. C. Sprott, W. J. C. Thio, Z. Y. Gu, A simple memristive jerk system, *IET Circ. Device. Syst.*, **15** (2021), 388–392. https://doi.org/10.1049/CDS2.12035
53. H. G. Tian, Z. Wang, P. J. Zhang, M. S. Chen, Y. Wang, Dynamic analysis and robust control of a chaotic system with hidden attractor, *Complexity*, **2021** (2021), 1–11. https://doi.org/10.1155/2021/8865522
54. S. Jafari, J. C. Sprott, S. M. R. H. Golpayegani, Elementary quadratic chaotic flows with no equilibria, *Phys. Lett. A*, **377** (2013), 699–702. https://doi.org/10.1016/j.physleta.2013.01.009
55. S. Zhang, Y. C. Zeng, A simple jerk-like system without equilibrium: Asymmetric coexisting hidden attractors, bursting oscillation and double full feigenbaum remerging trees, *Chaos Solitons Fract.*, **120** (2019), 25–40. https://doi.org/10.1016/j.chaos.2018.12.036
56. K. Rajagopal, S. T. Kingni, G. H. Kom, V. T. Pham, A. Karthikeyan, S. Jafari, Self-excited and hidden attractors in a simple chaotic jerk system and in its time-delayed form: Analysis, electronic implementation, and synchronization, *J. Korean Phys. Soc.*, **77** (2020), 145–152. https://doi.org/10.3938/jkps.77.145
57. J. Guckenheimer, P. Holmes, *Nonlinear oscillation, dynamical systems, and bifurcations of vector fields*, New York: Springer, 1983. https://doi.org/10.1007/978-1-4612-1140-2
58. L. Perko, *Differential equations and dynamical systems*, New York: Springer, 2001. https://doi.org/10.1007/978-1-4613-0003-8
59. B. D. Hassard, N. D. Kazarinoff, Y. H. Wan, *Theory and applications of Hopf bifurcation*, Cambridge: Cambridge University Press, 1981.
60. Y. A. Kuznetsov, *Elements of applied bifurcation theory*, New York: Springer, 1998.
61. B. Sang, B. Huang, Bautin bifurcations of a financial system, *Electron. J. Qual. Theory Differ. Equ.*, **2017** (2017), 1–22. https://doi.org/10.14232/ejqtde.2017.1.95
62. B. Sang, Focus quantities with applications to some finite-dimensional systems, *Math. Methods Appl. Sci.*, **44** (2021), 464–475. https://doi.org/10.1002/mma.6750
63. T. Asada, W. Semmler, Growth and finance: An intertemporal model, *J. Macroeconom.*, **17** (1995), 623–649. https://doi.org/10.1016/0164-0704(95)80086-7